Molecular nature of $P_{cs}(4459)$ and its heavy quark spin partners

C. W. Xiao,[1,*] J. J. Wu,[2,†] and B. S. Zou[3,2,1,‡]

[1]*School of Physics and Electronics, Central South University, Changsha 410083, China*
[2]*School of Physical Sciences, University of Chinese Academy of Sciences (UCAS), Beijing 100049, China*
[3]*Key Laboratory of Theoretical Physics, Institute of Theoretical Physics, Chinese Academy of Sciences, Beijing 100190, China*

(Received 9 February 2021; accepted 22 February 2021; published 17 March 2021)

Inspired by the observation of the $P_{cs}(4459)$ state by LHCb recently, we reexamine the results of the interaction of the $J/\psi\Lambda$ channel with its coupled channels, exploiting the coupled channel unitary approach combined with heavy quark spin and local hidden gauge symmetries. By tuning the only free parameter, we find a pole of $(4459.07 + i6.89)$ MeV below the $\bar{D}^*\Xi_c$ threshold, which was consistent with the mass and width of the $P_{cs}(4459)$ state. Thus, we assume the $P_{cs}(4459)$ state to be a $\bar{D}^*\Xi_c$ bound state with the possible degeneracy of $J^P = \frac{1}{2}^-$ and $J^P = \frac{3}{2}^-$. According to this degeneracy, it would have a two-pole structure, like $P_c(4450)$ before. There is another pole in the $J^P = \frac{1}{2}^-$ sector, $(4310.53 + i8.23)$ MeV, corresponding to a deep bound state of $\bar{D}\Xi_c$. Furthermore, the previously predicted loosely bound states $\bar{D}\Xi_c'$, $\bar{D}^*\Xi_c'$, $\bar{D}^*\Xi_c^*$ with $J = 1/2, I = 0$ and $\bar{D}^*\Xi_c'$, $\bar{D}\Xi_c^*$, $\bar{D}^*\Xi_c^*$ with $J = 3/2, I = 0$ may exist as either bound states or unbound virtual states. We hope that future experiments can search for the $\bar{D}^{(*)}\Xi_c$ molecular states not only in their dominant decay channels $\bar{D}_s^{(*)}\Lambda_c$, but also in the channels $J/\psi\Lambda$ and $\eta_c\Lambda$ in order to reveal their different natures.

DOI: 10.1103/PhysRevD.103.054016

I. INTRODUCTION

Using the coupled channel unitary approach (CCUA) [1–3] and the local hidden gauge (LHG) formalism [4–7] combined with SU(4) symmetry in early 2010, Ref. [8] shows that several hidden charm and hidden charm strangeness resonances were predicted around the energy range of 4200 MeV–4600 MeV, where the possible decay channel of $\eta_c N$ or $J/\psi N$ was suggested for the search for the hidden charm states in experiments. Its further investigation was given in detail in Ref. [9]. After that, the pentaquark states attracted theoretical interest once again with many predictions in the hidden charm sector [10–17]. In 2015, the LHCb Collaboration reported two pentaquark-like resonances found in the $J/\psi p$ invariant mass distributions of the $\Lambda_b^0 \to J/\psi K^- p$ decay [18,19], denoted as $P_c(4380)^+$ with a large width of 205 MeV and $P_c(4450)^+$ with a small width of 39 MeV, which were confirmed by a model-independent reanalysis of the experimental data [20] and in the $\Lambda_b^0 \to J/\psi p\pi^-$ decay [21]. Furthermore, in 2019 with the Run-2 data, the LHCb Collaboration updated the new results for the P_c states as three clear narrow structures [22]:

$$\begin{aligned} M_{P_{c1}} &= (4311.9 \pm 0.7^{+6.8}_{-0.6})\ \text{MeV}, \\ \Gamma_{P_{c1}} &= (9.8 \pm 2.7^{+3.7}_{-4.5})\ \text{MeV}, \\ M_{P_{c2}} &= (4440.3 \pm 1.3^{+4.1}_{-4.7})\ \text{MeV}, \\ \Gamma_{P_{c2}} &= (20.6 \pm 4.9^{+8.7}_{-10.1})\ \text{MeV}, \\ M_{P_{c3}} &= (4457.3 \pm 0.6^{+4.1}_{-1.7})\ \text{MeV}, \\ \Gamma_{P_{c3}} &= (6.4 \pm 2.0^{+5.7}_{-1.9})\ \text{MeV}, \end{aligned}$$

where the $P_c(4450)$ was split into two states of $P_c(4440)$ and $P_c(4457)$, in addition to a new narrow resonance $P_c(4312)$. However, the broad former resonance $P_c(4380)$ could neither be confirmed nor refuted in the updated results.

In principle, due to the fact that the P_c states were found in the experiments, the P_{cs} states as their strangeness partners should also exist as predicted in Refs. [8,9] from SU(4) flavor symmetry. Note that the first predictions for the masses and the widths of the molecular resonances in Refs. [8,9] were influenced by the experimental information to determine the only free parameter of a_μ (μ is not an independent energy scale parameter [3,23,24]) in the loop

*xiaochw@csu.edu.cn
†wujiajun@ucas.ac.cn
‡zoubs@itp.ac.cn

functions. Therefore, after the updated results of the LHCb Collaboration [22] became available, this free parameter was fitted as $a_\mu(\mu = 1\ \text{GeV}) = -2.09$ in Ref. [25] with the masses of three P_c states based on Ref. [15], where seven hidden charm molecular states were predicted using the CCUA and LHG formalism together with the heavy quark spin symmetry (HQSS) [26–28]. Inspired by the experimental findings of the P_c states, with the same fitted parameter of a_μ from the P_c states, using the LHG and HQSS, several bound states of $\bar{D}^{(*)}\Xi_c^{(*)}$ and $\bar{D}^{(*)}\Xi_c'$ were predicted in Ref. [29], where some of them were analogous to the bound states in Refs. [8,9]. At the end of Ref. [29] as well as in Refs. [30,31] it was recommended to look for these states in the reaction $\Xi_b^- \to J/\psi\Lambda K^-$. The possibility to look for these states in the Λ_b decays was also discussed in Refs. [32,33]. Furthermore, the decay properties of the hidden charm strangeness resonances predicted in Refs. [8,9] were investigated in detail in Ref. [34], where the partial decay widths of possible decay channels were obtained by exploiting the effective Lagrangian framework through the triangle loops. On the other hand, with the one-boson-exchange model, Ref. [35] also predicted that the possible $\bar{D}_s^*\Sigma_c^{(*)}$ and $\bar{D}^*\Xi_c^{(\prime,)}$ pentaquark states existed. Taking into account the spin-flavor symmetric states, the possible $SU_f(3)$ multiplets for the charmonium compact pentaquark states were obtained in Ref. [31], where the possible decay channels and the partial decay widths were discussed for these predictions. Using the chiral effective field theory up to the next-to-leading order, Ref. [36] found ten bound states in the hidden charm strangeness systems of $\bar{D}^{(*)}\Xi_c'$ and $\bar{D}^{(*)}\Xi_c^{(*)}$ with different spin, where a mass difference of about 6 MeV for two $\bar{D}^*\Xi_c$ molecular states with spins $J = \frac{1}{2}$ and $J = \frac{3}{2}$ was obtained and looking for these P_{cs} states in the decay channel of $J/\psi\Lambda$ was suggested.

Just recently, the LHCb Collaboration had reported the results of the $\Xi_b^- \to J/\psi\Lambda K^-$ decay in Ref. [37], where a resonance structure of the $P_{cs}(4459)$ state was found in the invariant mass distributions of $J/\psi\Lambda$, given as

$$M_{P_{cs}} = (4458.8 \pm 2.9^{+4.7}_{-1.1})\ \text{MeV},$$
$$\Gamma_{P_{cs}} = (17.3 \pm 6.5^{+8.0}_{-5.7})\ \text{MeV},$$

which is just about 19 MeV below the $\bar{D}^{*0}\Xi_c^0$ threshold. Note that, analogous to the degenerate $P_c(4450)$ state, for the current data sample a prediction of the spin structure in Refs. [29,36] was combined with a large uncertainty. The two-pole structure was also suggested in the results of the QCD sum rules in Ref. [38], where the $P_{cs}(4459)$ state was assumed to be a $\bar{D}^*\Xi_c$ molecular state with spin-parity $J^P = \frac{1}{2}^-$ or $J^P = \frac{3}{2}^-$, and a $\bar{D}\Xi_c$ bound state at $4.29^{+0.13}_{-0.12}$ GeV with $J^P = \frac{1}{2}^-$ was found, too. Again, with the QCD sum rules, Ref. [39] assigned the $P_{cs}(4459)$ state as a hidden charm compact pentaquark state with $J^P = \frac{1}{2}^-$, which was confirmed later in Refs. [40,41]. On the other hand, with a combined effective field theory and phenomenological assumptions, Ref. [42] proposed that the $P_{cs}(4459)$ state could more likely be a $\bar{D}^*\Xi_c$ molecular pentaquark state with $J^P = \frac{3}{2}^-$, or possibly $J^P = \frac{1}{2}^-$ with more uncertainties about its mass. Using a coupled channel analysis based on the one-boson-exchange model, Ref. [43] concluded that the $P_{cs}(4459)$ state was not a pure $\bar{D}^*\Xi_c$ molecular state and that other possible resonances of $\bar{D}^{(*)}\Xi_c^{(\prime,*)}$ could exist, and its decay behavior was further discussed in Ref. [44]. Using effective field theory by taking into account the HQSS and SU(3) flavor symmetry, in Ref. [45] the existence of the $\bar{D}^{(*)}\Xi_c^{(\prime,*)}$ molecular states were also found, which were the SU(3)-flavor partners of the $\bar{D}^{(*)}\Sigma_c^{(*)}$ molecular states. With the quasipotential Bethe-Salpeter equation approach, Ref. [46] assigned the $P_{cs}(4459)$ state to the $\bar{D}^*\Xi_c$ molecular state with $J^P = \frac{3}{2}^-$ and predicted other $\bar{D}^{(*)}\Xi_c^{(\prime,*)}$ states with different spins. Furthermore, the $P_{cs}(4459)$ state was suggested to be searched for in the decay $\Lambda_b \to J/\psi\Lambda\phi$ in Ref. [47].

Motivated by the new findings of Ref. [37], we reexamine the results of Refs. [8,9,29] to understand the differences between our predictions and experimental data. We fix the model parameters to make further predictions.

II. FORMALISM

There are various approaches to dealing with hadronic molecules as recently reviewed in Refs. [48,49]. The LHG formalism seems to be working well to give a general consistent explanation for various observed hadronic molecular candidates with hidden charm [50,51]. In Ref. [29], combining the CCUA with the LHG formalism, we considered the coupled channels of the $J/\psi\Lambda$ channel, where there were nine channels ($\eta_c\Lambda$, $J/\psi\Lambda$, $\bar{D}\Xi_c$, $\bar{D}_s\Lambda_c$, $\bar{D}\Xi_c'$, $\bar{D}^*\Xi_c$, $\bar{D}_s^*\Lambda_c$, $\bar{D}^*\Xi_c'$, $\bar{D}^*\Xi_c^*$) in the $J^P = \frac{1}{2}^-, I = 0$ sector, and six channels ($J/\psi\Lambda$, $\bar{D}^*\Xi_c$, $\bar{D}_s^*\Lambda_c$, $\bar{D}^*\Xi_c'$, $\bar{D}\Xi_c^*$, $\bar{D}^*\Xi_c^*$) in the $J^P = \frac{3}{2}^-, I = 0$ sector. In addition, using the HQSS, a single channel of $\bar{D}^*\Xi_c^*$ with $J^P = \frac{5}{2}^-$ was also found in the s wave, which was not taken into account in our work since it could not couple to the $J/\psi\Lambda$ channel in the s wave. Note that the interaction of the $\bar{D}^*\Xi_c^*$ channel, which can be specified with spin $J = \frac{1}{2}, \frac{3}{2}, \frac{5}{2}$, was included in the coupled channels in Ref. [29] under the constraint of the HQSS, and not considered in Refs. [8,9].

Within the CCUA, the scattering amplitudes (T) are evaluated by the coupled channel Bethe-Salpeter equation with the on-shell prescription,

$$T = [1 - VG]^{-1}V, \tag{1}$$

where G is constructed by the loop functions with meson-baryon intermediate states and V are the potentials of the

TABLE I. Potential matrix elements V_{ij} of Eq. (1) for the sector $J = 1/2, I = 0$.

$\eta_c\Lambda$	$J/\psi\Lambda$	$\bar{D}\Xi_c$	$\bar{D}_s\Lambda_c$	$\bar{D}\Xi_c'$	$\bar{D}^*\Xi_c$	$\bar{D}_s^*\Lambda_c$	$\bar{D}^*\Xi_c'$	$\bar{D}^*\Xi_c^*$
μ_1	0	$-\frac{1}{2}\mu_{12}$	$-\frac{1}{2}\mu_{13}$	$\frac{1}{2}\mu_{14}$	$\frac{\sqrt{3}}{2}\mu_{12}$	$\frac{\sqrt{3}}{2}\mu_{13}$	$\frac{1}{2\sqrt{3}}\mu_{14}$	$\sqrt{\frac{2}{3}}\mu_{14}$
	μ_1	$\frac{\sqrt{3}}{2}\mu_{12}$	$\frac{\sqrt{3}}{2}\mu_{13}$	$\frac{1}{2\sqrt{3}}\mu_{14}$	$\frac{1}{2}\mu_{12}$	$\frac{1}{2}\mu_{13}$	$\frac{5}{6}\mu_{14}$	$-\frac{\sqrt{2}}{3}\mu_{14}$
		μ_2	μ_{23}	0	0	0	$\frac{1}{\sqrt{3}}\mu_{24}$	$-\sqrt{\frac{2}{3}}\mu_{24}$
			μ_3	0	0	0	$\frac{1}{\sqrt{3}}\mu_{34}$	$-\sqrt{\frac{2}{3}}\mu_{34}$
				$\frac{1}{3}(2\lambda+\mu_4)$	$\frac{1}{\sqrt{3}}\mu_{24}$	$\frac{1}{\sqrt{3}}\mu_{34}$	$-\frac{2}{3\sqrt{3}}(\lambda-\mu_4)$	$\frac{1}{3}\sqrt{\frac{2}{3}}(\mu_4-\lambda)$
					μ_2	μ_{23}	$\frac{2}{3}\mu_{24}$	$\frac{\sqrt{2}}{3}\mu_{24}$
						μ_3	$\frac{2}{3}\mu_{34}$	$\frac{\sqrt{2}}{3}\mu_{34}$
							$\frac{1}{9}(2\lambda+7\mu_4)$	$\frac{\sqrt{2}}{9}(\lambda-\mu_4)$
								$\frac{1}{9}(\lambda+8\mu_4)$

coupled channel interactions. Note that G is a diagonal matrix with elements of meson-baryon loop functions, where we take the ones with the dimensional regularization (see more details in Refs. [8,9]). Thus, a_μ is the only free parameter, see the discussions later for examples. Respecting the HQSS, the elements of the potential V matrix are given in Tables I and II for the $J = 1/2, I = 0$ and $J = 3/2, I = 0$ sectors, respectively, where we only show V_{ij} for $j \geq i$ for simplicity due to the fact that $V_{ji} = V_{ij}$ in the CCUA. In Tables I and II, the coefficients μ_i, μ_{ij} $(i, j = 1, 2, 3, 4)$, and λ are the unknown low energy constants with the HQSS constraint (see more details in Ref. [29]).

Using the LHG formalism, we obtain the values of these low energy constants [29],

$$\mu_1 = \mu_3 = \mu_{24} = \mu_{34} = 0, \tag{2}$$

$$\mu_2 = \mu_{23}/\sqrt{2} = \mu_4 = \lambda = -F, \quad F = \frac{1}{4f^2}(p^0 + p'^0), \tag{3}$$

$$\mu_{12} = -\mu_{13}/\sqrt{2} = \mu_{14}/\sqrt{3} = -\sqrt{\frac{2}{3}}\frac{m_V^2}{m_{D^*}^2}F, \tag{4}$$

TABLE II. Potential matrix elements V_{ij} of Eq. (1) for the sector $J = 3/2, I = 0$.

$J/\psi\Lambda$	$\bar{D}^*\Xi_c$	$\bar{D}_s^*\Lambda_c$	$\bar{D}^*\Xi_c'$	$\bar{D}\Xi_c^*$	$\bar{D}^*\Xi_c^*$
μ_1	μ_{12}	μ_{13}	$-\frac{1}{3}\mu_{14}$	$\frac{1}{\sqrt{3}}\mu_{14}$	$\frac{\sqrt{5}}{3}\mu_{14}$
	μ_2	μ_{23}	$-\frac{1}{3}\mu_{24}$	$\frac{1}{\sqrt{3}}\mu_{24}$	$\frac{\sqrt{5}}{3}\mu_{24}$
		μ_3	$-\frac{1}{3}\mu_{34}$	$\frac{1}{\sqrt{3}}\mu_{34}$	$\frac{\sqrt{5}}{3}\mu_{34}$
			$\frac{1}{9}(8\lambda+\mu_4)$	$\frac{1}{3\sqrt{3}}(\lambda-\mu_4)$	$\frac{\sqrt{5}}{9}(\lambda-\mu_4)$
				$\frac{1}{3}(2\lambda+\mu_4)$	$\frac{1}{3}\sqrt{\frac{5}{3}}(\mu_4-\lambda)$
					$\frac{1}{9}(4\lambda+5\mu_4)$

with $f_\pi = 93$ MeV and $m_V = 800$ MeV, where p^0 and p'^0 are the energies of the incoming and outgoing mesons in a certain channel. Note that we have explicitly used the reduction factor $m_V^2/m_{D^*}^2$ in the matrix elements that involve the transition processes with the exchange of a D^* meson. The zero values for μ_{24} and μ_{34} are due to the neglect of pion exchange in our formalism, as seen in Ref. [15]. See more discussions in Ref. [24].

III. RESULTS AND DISCUSSIONS

As discussed above, the subtraction constant a_μ in the meson-baryon loop functions is a free parameter in our formalism, and thus, we cannot get a precise value for it theoretically. It is even worse that the prediction will significantly rely on the value of a_μ in a loosely bound way, since the value of this parameter will influence the lowest strength of attractive potential to form a bound state (we will discuss this issue in detail later). In practice, the only way to get its accurate value is by using some experimental data to fix it. Therefore, using the newest experimental results of Ref. [37], the value of a_μ can be determined as $a_\mu(\mu = 1\ \text{GeV}) = -1.94$ for the P_{cs} case. It is similar to what we have done in Ref. [25] for the P_c case, where a value of $a_\mu(\mu = 1\ \text{GeV}) = -2.09$ was obtained. In the early prediction of Refs. [8,9], the central value of $a_\mu(\mu = 1\ \text{GeV}) = -2.3$ was used to match the cutoff in the loop function as 0.8 GeV, which is close to the masses of the exchanged vector mesons ρ and ω. Indeed, now the values of $a_\mu(\mu = 1\ \text{GeV}) = -1.94$ and the one of $a_\mu(\mu = 1\ \text{GeV}) = -2.09$ [25] are really surrounding the "natural values" $a_\mu = -2$ [3].

Using the fitted $a_\mu(\mu = 1\ \text{GeV}) = -1.94$, we obtain the results of the modulus squared of the amplitudes in Figs. 1 and 2 for the $J = 1/2, I = 0$ and $J = 3/2, I = 0$ sectors, respectively, where the peak structures are analogous to the ones obtained in Ref. [29] but more narrow and with higher

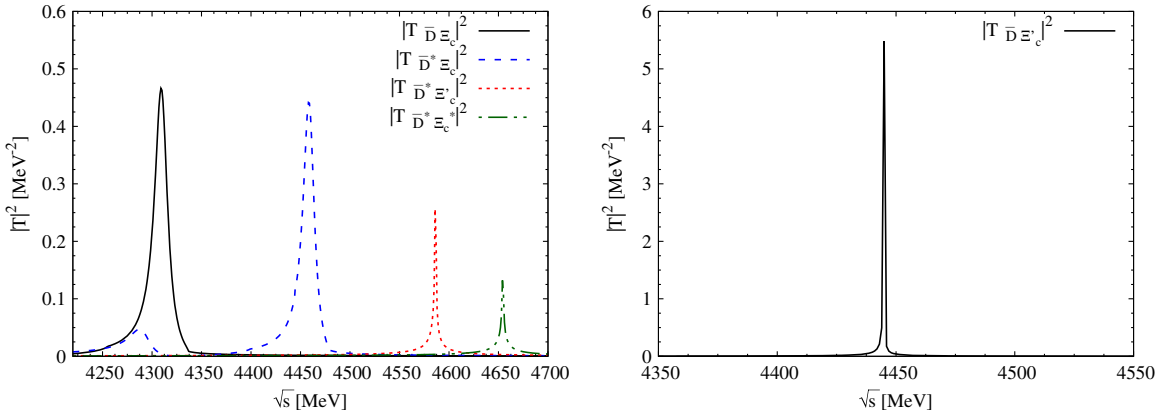

FIG. 1. Results of the modulus squared of the amplitudes for the sector $J = 1/2, I = 0$.

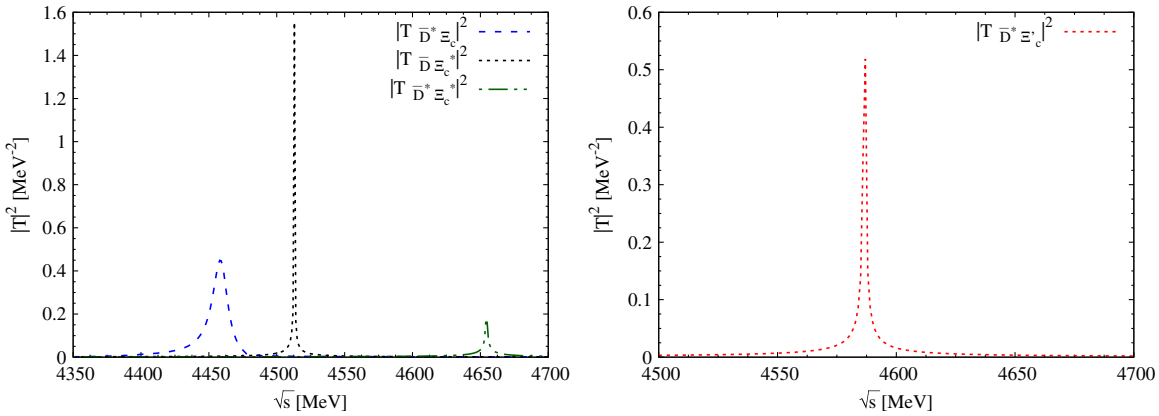

FIG. 2. Results of the modulus squared of the amplitudes for the sector $J = 3/2, I = 0$.

energies. The corresponding poles and its coupling constants to all the channels are given in Tables III[1] and IV for the $J = 1/2, I = 0$ and $J = 3/2, I = 0$ sectors, respectively, where the thresholds of each channel are shown accordingly. In Tables III and IV, with the couplings obtained, the partial decay widths and the branching ratios for each channel are evaluated. Note that the poles given in Tables III and IV are the ones located in the general "second Riemann sheet," which means that all the channels below the certain bound channel are extrapolated to the second Riemann sheet (these channels are always called the open channels), whereas the other coupled channels including the bound channel are in the first Riemann sheet. As found from our results in Tables III and IV, the bound state of $\bar{D}^*\Xi_c$ is tuned as 4459 MeV to make it consistent with the mass of the observed P_{cs} state, which has increased by about 30 MeV with respect to the one obtained in Ref. [29]. Accordingly, the pole of the $\bar{D}^*\Xi_c$ channel is found at $(4459.07 + i6.89)$ MeV, where the width (encoded by the imaginary part) is quite consistent with the experimental results [37], showing only a 3 MeV difference. Note that, owing to the pion exchange neglect in our formalism as discussed above, this pole of the $\bar{D}^*\Xi_c$ channel is degenerate with spins $J = 1/2$ and $J = 3/2$, as shown in Tables III and IV. Therefore, one can conclude from our formalism that the $P_{cs}(4459)$ state can be a bound state of $\bar{D}^*\Xi_c$ with spin uncertainty of $J = 1/2$ or $J = 3/2$. Besides, in Table III for the $J = 1/2, I = 0$ sector, we have another very stable pole, $(4310.53 + i8.23)$ MeV, which is bound by the $\bar{D}\Xi_c$ channel and has 56 MeV binding energy. On the other hand, the other three peak structures are very close to the corresponding thresholds. The peak at around 4445 MeV is contributed by the pole at $(4445.12 + i0.19)$ MeV bound by the $\bar{D}\Xi'_c$ channel, of which the binding energy is just 0.23 MeV. Thus, in our

[1]There is an extra pole around $(4291.05 + i12.80)$ MeV in the $\bar{D}^*\Xi_c$ channel, see the left panel of Fig. 1, which couples strongly to the $\bar{D}_s^*\Lambda_c$ channel (threshold 4398.66 MeV) and looks strange. This pole is due to the fact that the G functions for the channels $\bar{D}^*\Xi_c$ and $\bar{D}_s^*\Lambda_c$ (denoted as channels 6 and 7, respectively) become positive far below their thresholds, which also leads to the "effective" potential of $V_{66} + V_{67}^2 G_{77}$ changing to a positive one (see the discussion later). Thus, a repulsive potential leads to an unusual bound state. See more discussions in Refs. [15,52].

TABLE III. Coupling constants to all channels for certain poles in the sector $J = 1/2, I = 0$.

Chan.	$\eta_c\Lambda$	$J/\psi\Lambda$	$\bar{D}\Xi_c$	$\bar{D}_s\Lambda_c$	$\bar{D}\Xi_c'$	$\bar{D}^*\Xi_c$	$\bar{D}_s^*\Lambda_c$	$\bar{D}^*\Xi_c'$	$\bar{D}^*\Xi_c^*$
Thres.	4099.58	4212.58	4366.61	4254.80	4445.34	4477.92	4398.66	4586.66	4654.48
$4310.53 + i8.23$									
$\lvert g_i\rvert$	0.15	0.27	**2.33**	0.69	0.00	0.04	0.09	0.01	0.02
Γ_i	0.57	1.18	⋯	13.86	⋯	⋯	⋯	⋯	⋯
Br.	3.47%	7.16%	⋯	84.21%	⋯	⋯	⋯	⋯	⋯
$4445.12 + i0.19$									
$\lvert g_i\rvert$	0.10	0.06	0.00	0.00	**0.72**	0.08	0.04	0.01	0.01
Γ_i	0.29	0.08	0.00	0.00	⋯	⋯	0.04	⋯	⋯
Br.	74.74%	21.22%	0.01%	0.01%	⋯	⋯	10.62%	⋯	⋯
$4459.07 + i6.89$									
$\lvert g_i\rvert$	0.22	0.13	0.00	0.00	0.07	**2.16**	0.61	0.03	0.02
Γ_i	1.59	0.46	0.00	0.00	0.01	⋯	11.14	⋯	⋯
Br.	11.57%	3.31%	0.00%	0.00%	0.70%	⋯	80.86%	⋯	⋯
4586.66?									
$\lvert g_i\rvert$	⋯	⋯	⋯	⋯	⋯	⋯	⋯	⋯	⋯
4654.48?									
$\lvert g_i\rvert$	⋯	⋯	⋯	⋯	⋯	⋯	⋯	⋯	⋯

TABLE IV. Coupling constants to all channels for certain poles in the sector $J = 3/2, I = 0$.

Chan.	$J/\psi\Lambda$	$\bar{D}^*\Xi_c$	$\bar{D}_s^*\Lambda_c$	$\bar{D}^*\Xi_c'$	$\bar{D}\Xi_c^*$	$\bar{D}^*\Xi_c^*$
Thres.	4212.58	4477.92	4398.66	4586.66	4513.17	4654.48
$4459.02 + i6.83$						
$\lvert g_i\rvert$	0.28	**2.16**	0.61	0.02	0.04	0.03
Γ_i	2.00	⋯	11.15	⋯	⋯	⋯
Br.	14.68%	⋯	81.64%	⋯	⋯	⋯
4586.66?						
$\lvert g_i\rvert$	⋯	⋯	⋯	⋯	⋯	⋯
4513.17?						
$\lvert g_i\rvert$	⋯	⋯	⋯	⋯	⋯	⋯
4654.48?						
$\lvert g_i\rvert$	⋯	⋯	⋯	⋯	⋯	⋯

model this bound state becomes unstable if the parameter a_μ changes a little to move this pole to the threshold, leading to a threshold effect with no pole in the general second Riemann sheet, as shown in Tables III and IV for some channels. Furthermore, the other two peak structures are actually due to the poles from the other Riemann sheets. Thus, these poles cannot be recognized as normal bound states of the certain channels. It is proper to say that these two peak structures are threshold effects because of very weak attractive interaction potentials. Indeed, the three poles for the channels $\bar{D}\Xi_c'$, $\bar{D}^*\Xi_c'$, and $\bar{D}^*\Xi_c^*$ were just loosely bound as found in the results of Ref. [29], where these poles were only a few MeV below the corresponding thresholds and had narrow widths of a few MeV. Similarly, in Table IV for the $J = 3/2, I = 0$ sector, except for the stable pole of $\bar{D}^*\Xi_c$, the other three poles of the channels $\bar{D}^*\Xi_c'$, $\bar{D}\Xi_c^*$, and $\bar{D}^*\Xi_c^*$ are not stable for the same reason. Three of them were also loosely bound as given in the results of Ref. [29] with a few MeV for the binding energies and the widths.

As shown in Tables III and IV, the degenerate molecular states of $\bar{D}^*\Xi_c$ with $J = 1/2$ and $J = 3/2$ correspond to nearly the same pole, $(4459.07 + i6.89)$ MeV. Their main decay channel is $\bar{D}_s^*\Lambda_c$ with the branching ratio being larger than 80%. This can be understood in our model, as this channel comes from the strong interaction by exchanging a light vector meson, and its large decay width was also found in Ref. [44]. However, the branching ratios of the $J/\psi\Lambda$ channel in the two cases are a little different because of the Clebsch-Gordan coefficients in the HQSS model. Besides, the $\eta_c\Lambda$ channel is the only decay channel of the bound state with $J^P = 1/2^-$ while it requires the d wave interaction for the $J^P = 3/2^-$ state, which is neglected in our model. Therefore, if we assume the $\bar{D}^*\Xi_c$ bound state to be the $P_{cs}(4459)$ state, it may have a two-pole structure with different spins, like the one of $P_c(4450)$ before, and it

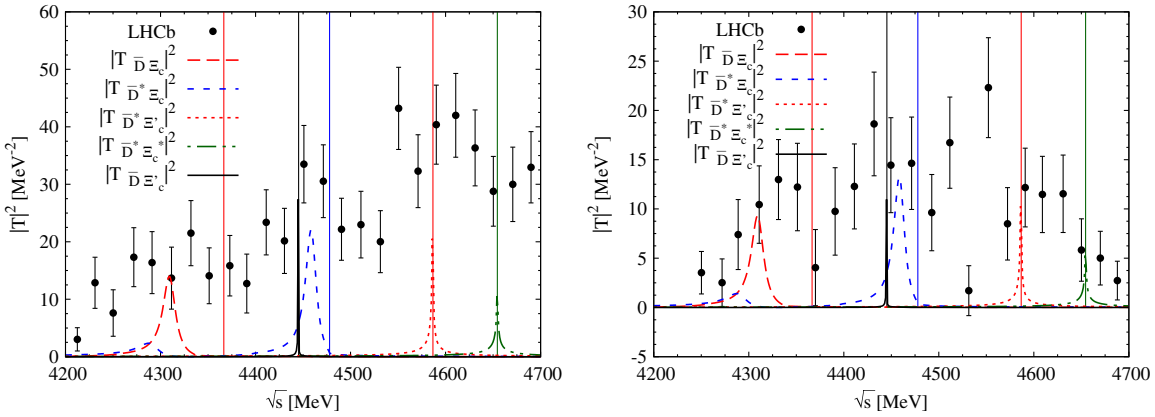

FIG. 3. Results of the modulus squared of the amplitudes for the sector $J = 1/2, I = 0$ compared with the experimental data, Left: with full data; Right: with 1.9 GeV $< m_{\Lambda K^-} <$ 2.2 GeV. The vertical lines correspond to the thresholds of the different channels.

can be helpful to reveal the nature of these two poles in the future with more experimental information for the partial decay widths and the branching ratios of the channels $J/\psi\Lambda$ and $\eta_c\Lambda$. In Fig. 3, we show our results of Fig. 1 for the $J = 1/2, I = 0$ sector compared to the experimental data, where the full data are compared on the left and the parts with the cut 1.9 GeV $< m_{\Lambda K^-} <$ 2.2 GeV on the right. As one can see from Fig. 3, the Run 2 data at hand do not provide enough statistics to draw a strong conclusion for the existence of more bound states in the $J/\psi\Lambda$ invariant mass distributions.

For the results of the partial decay widths and the branching ratios shown in Table III, it seems strange that the bound state of $\bar{D}\Xi_c$, with its pole at $(4310.53 + i8.23)$ MeV, decays more strongly to the $J/\psi\Lambda$ channel than to the $\eta_c\Lambda$ channel, while for the molecular state of $\bar{D}^*\Xi_c$ with pole $(4459.07 + i6.89)$ MeV it is just the opposite. This is different from the cases of the $\bar{D}^{(*)}\Sigma_c$ bound states studied in Ref. [24] because of the constraint of the HQSS, see the transition elements of $\frac{1}{2}\mu_{12}$ and $\frac{\sqrt{3}}{2}\mu_{12}$ for the related channels in Table I. In contrast to this, in Ref. [34] the bound state of $\bar{D}^*\Xi_c$ predicted in Refs. [8,9] was found to decay stronger in relation to the $J/\psi\Lambda$ channel than to the $\eta_c\Lambda$ channel. Indeed, Refs. [8,9,34] considered neither the HQSS nor the transition between Pseudoscalar-Baryon (PB) and Vector-Baryon (VB) channels. Taking into account the HQSS, the interactions between PB and VB channels are almost the same except for the Clebsch-Gordan coefficients. On the other hand, the bound states of $\bar{D}\Xi_c$ and $\bar{D}^*\Xi_c$ decay mostly to the channels $\bar{D}_s\Lambda_c$ and $\bar{D}_s^*\Lambda_c$, respectively, which have quite large partial decay widths and branching ratios (see the results in Tables III and IV), whereas the $\bar{D}^{(*)}\Sigma_c$ bound states [24] cannot decay to the channels $\bar{D}^{(*)}\Lambda_c$ via vector meson exchange. The reason is that the Λ_c particle is in the same spin 1/2 antitriplet (the multistates $\bar{3}$) with the Ξ_c particle under SU(3) flavor symmetry, but not with the Σ_c particle (belonging to the multistates 6).

As discussed above, when we take the new value of $a_\mu(\mu = 1\ \text{GeV}) = -1.94$ for the only free parameter in the loop functions, the loosely bound systems $\bar{D}\Xi_c'$, $\bar{D}^*\Xi_c'$, $\bar{D}^*\Xi_c^*$ in the $J = 1/2, I = 0$ sector, and $\bar{D}^*\Xi_c'$, $\bar{D}\Xi_c^*$, $\bar{D}^*\Xi_c^*$ in the $J = 3/2, I = 0$ sector, have become unstable with the

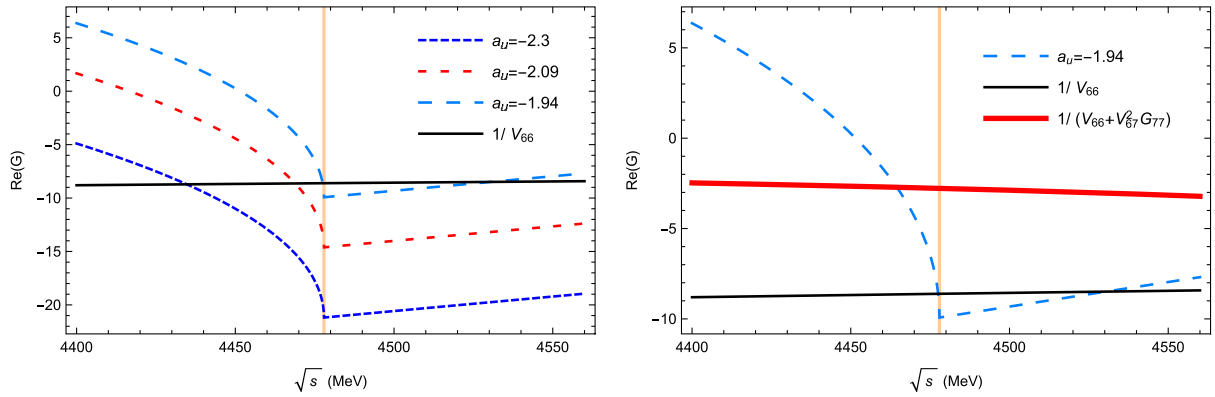

FIG. 4. Results for the inverse potential $1/V_{66}$ (solid lines) versus the real parts of the loop function (dashed lines) for the $\bar{D}^*\Xi_c$ channel, where the vertical line indicates the location of the threshold and the channels 6, and 7 in the lower indexes, denote the channels $\bar{D}^*\Xi_c$, and $\bar{D}_s^*\Lambda_c$, respectively.

poles moving to the thresholds, except for three strongly bound systems $\bar{D}\Xi_c$ and $\bar{D}^*\Xi_c$ (with $J = 1/2$ and $J = 3/2$). Note that all of these were considered as bound states in Ref. [29] with $a_\mu(\mu = 1\ \text{GeV}) = -2.09$, and even more bound with $a_\mu(\mu = 1\ \text{GeV}) = -2.3$ used in Refs. [8,9] (for example, $\bar{D}^*\Xi_c$ with pole at 4370 MeV which had been below the threshold of the $\bar{D}_s^*\Lambda_c$ channel). In fact, a reduced value of a_μ renders all of the poles to be less bound. Some of the loosely bound states moved to the thresholds. This is shown in the left part of Fig. 4, where we plot the real parts of the loop function G_{66}[2] with different a_μ and the inverse potential $1/V_{66}$, taking the $\bar{D}^*\Xi_c$ channel, for example (denoted as the channel 6 in the lower indexes in the figure). A more detailed discussion about the pole moving by the free parameter of the loop functions can be found in Refs. [53,54]. Furthermore, there is a strong coupling between the channels $\bar{D}^*\Xi_c$ (channel 6) and $\bar{D}_s^*\Lambda_c$ (referred to as the channel 7 in the lower indexes in the figure), indicating an off-diagonal transition potential which strengthens the attractive interaction via the coupled channel effect from pure diagonal potential V_{66} to the "effective" potential of $V_{66} + V_{67}^2 G_{77}$, owing to $V_{77} = \mu_3 = 0$ [see Table I and Eq. (2)]. In the right panel of Fig. 4, we compare the real parts of the loop function G_{66} with $1/V_{66}$ and $1/(V_{66} + V_{67}^2 G_{77})$ (taking $a_\mu = -1.94$), where the intersection point indicates the pole position. Thus, one can expect that the $\bar{D}^*\Xi_c$ system will be more bound when $a_\mu(\mu = 1\ \text{GeV}) = -2.3$ is taken, as in Refs. [8,9], which is analogous to the case of the $\bar{D}\Xi_c$ system with the contribution from the $\bar{D}_s\Lambda_c$ channel.

IV. CONCLUSION

In summary, we revisited the interactions of the $J/\psi\Lambda$ channel and its coupled channels in the s wave, using the CCUA in combination with the LHG formalism and the HQSS. With the new observation of the $P_{cs}(4459)$ state by LHCb fixing the only free parameter, we obtain a pole at $(4459.07 + i6.89)$ MeV located below the threshold of the $\bar{D}^*\Xi_c$ channel, which represents effectively the two nearly degenerate states with spin parities $J^P = \frac{1}{2}^-$ and $J^P = \frac{3}{2}^-$ in our approach, keeping in the potential only the constant leading term while dropping the momentum dependent terms. To remove the degeneracy, in the future we will take into account the momentum dependent terms, including the pion exchange mechanism. Thus, by assuming the LHCb observed $P_{cs}(4459)$ peak to be the degenerated $\bar{D}^*\Xi_c$ molecular states from our formalism, it would split to two peaks with higher statistics in the future, like the previous $P_c(4450)$ peak observed by LHCb. From our results, there is also a $\bar{D}\Xi_c$ bound state with $J^P = \frac{1}{2}^-$ and a pole at $(4310.53 + i8.23)$ MeV, which is consistent with the predictions of Ref. [38] within the uncertainties. Owing to the uncertainties of the experimental data and hence their corresponding constraint to the free parameter, the possible loosely bound states $\bar{D}\Xi_c'$, $\bar{D}^*\Xi_c'$, $\bar{D}^*\Xi_c^*$ with $J = 1/2$, $I = 0$ and $\bar{D}^*\Xi_c'$, $\bar{D}\Xi_c^*$, $\bar{D}^*\Xi_c^*$ with $J = 3/2, I = 0$, which were predicted previously, are in fact suffering a large model dependence since there are no coupled channels to strengthen the attractive interaction. Unfortunately, in our present work even the existence of these states is put into question. Although the LHG potentials are attractive, it depends on the model parameter and the neglected momentum dependent terms whether they are bound states or virtual states. These results are consistent with a recent general analysis in Ref. [50]. To look for these molecular states, especially for the $\bar{D}\Xi_c$ bound state and two $\bar{D}^*\Xi_c$ states [corresponding to the observed $P_{cs}(4459)$ peak], the decay channels $\bar{D}_s\Lambda_c$ and $\bar{D}_s^*\Lambda_c$, respectively, are strongly suggested due to their large decay branching ratios. Searching for these states both in the $J/\psi\Lambda$ and $\eta_c\Lambda$ channels can be helpful to distinguish their different natures. We hope that future experiments, the Run-3 in LHCb for example, can make further tests on our predictions and suggestions to reveal the properties of the P_{cs} states.

[2]Note that below the threshold of a certain channel, the imaginary part of the loop function is zero.

ACKNOWLEDGMENTS

We thank Bo Fang for useful discussions and valuable comments on the experimental information, and acknowledge useful comments and careful reading of the paper by Eulogio Oset. This work is partly supported by the Fundamental Research Funds for the Central Universities (J. J. W.), and the NSFC under Grant No. 12070131001 (CRC110 cofunded by the DFG and NSFC), Grant No. 11835015, No. 12047503, and by the Chinese Academy of Sciences (CAS) under Grant No. XDB34030000 (B. S. Z.).

[1] J. A. Oller and E. Oset, Nucl. Phys. **A620**, 438 (1997); **A652**, 407(E) (1999).
[2] E. Oset and A. Ramos, Nucl. Phys. **A635**, 99 (1998).
[3] J. A. Oller and U.-G. Meißner, Phys. Lett. B **500**, 263 (2001).
[4] M. Bando, T. Kugo, S. Uehara, K. Yamawaki, and T. Yanagida, Phys. Rev. Lett. **54**, 1215 (1985).
[5] M. Bando, T. Kugo, and K. Yamawaki, Phys. Rep. **164**, 217 (1988).
[6] U.-G. Meißner, Phys. Rep. **161**, 213 (1988).
[7] H. Nagahiro, L. Roca, A. Hosaka, and E. Oset, Phys. Rev. D **79**, 014015 (2009).
[8] J. J. Wu, R. Molina, E. Oset, and B. S. Zou, Phys. Rev. Lett. **105**, 232001 (2010).
[9] J. J. Wu, R. Molina, E. Oset, and B. S. Zou, Phys. Rev. C **84**, 015202 (2011).
[10] W. L. Wang, F. Huang, Z. Y. Zhang, and B. S. Zou, Phys. Rev. C **84**, 015203 (2011).
[11] Z. C. Yang, Z. F. Sun, J. He, X. Liu, and S. L. Zhu, Chin. Phys. C **36**, 6 (2012).
[12] S. G. Yuan, K. W. Wei, J. He, H. S. Xu, and B. S. Zou, Eur. Phys. J. A **48**, 61 (2012).
[13] J. J. Wu, T.-S. H. Lee, and B. S. Zou, Phys. Rev. C **85**, 044002 (2012).
[14] C. García-Recio, J. Nieves, O. Romanets, L. L. Salcedo, and L. Tolos, Phys. Rev. D **87**, 074034 (2013).
[15] C. W. Xiao, J. Nieves, and E. Oset, Phys. Rev. D **88**, 056012 (2013).
[16] T. Uchino, W. H. Liang, and E. Oset, Eur. Phys. J. A **52**, 43 (2016).
[17] M. Karliner and J. L. Rosner, Phys. Rev. Lett. **115**, 122001 (2015).
[18] R. Aaij *et al.* (LHCb Collaboration), Phys. Rev. Lett. **115**, 072001 (2015).
[19] R. Aaij *et al.* (LHCb Collaboration), Chin. Phys. C **40**, 011001 (2016).
[20] R. Aaij *et al.* (LHCb Collaboration), Phys. Rev. Lett. **117**, 082002 (2016).
[21] R. Aaij *et al.* (LHCb Collaboration), Phys. Rev. Lett. **117**, 082003 (2016).
[22] R. Aaij *et al.* (LHCb Collaboration), Phys. Rev. Lett. **122**, 222001 (2019).
[23] A. Ozpineci, C. W. Xiao, and E. Oset, Phys. Rev. D **88**, 034018 (2013).
[24] C. W. Xiao, J. X. Lu, J. J. Wu, and L. S. Geng, Phys. Rev. D **102**, 056018 (2020).
[25] C. W. Xiao, J. Nieves, and E. Oset, Phys. Rev. D **100**, 014021 (2019).
[26] N. Isgur and M. B. Wise, Phys. Lett. B **232**, 113 (1989).
[27] M. Neubert, Phys. Rep. **245**, 259 (1994).
[28] A. V. Manohar and M. B. Wise, *Heavy Quark Physics*, Cambridge Monographs on Particle Physics, Nuclear Physics and Cosmology, Vol. 10 (Cambridge University Press, Cambridge, England, 2000).
[29] C. W. Xiao, J. Nieves, and E. Oset, Phys. Lett. B **799**, 135051 (2019).
[30] H. X. Chen, L. S. Geng, W. H. Liang, E. Oset, E. Wang, and J. J. Xie, Phys. Rev. C **93**, 065203 (2016).
[31] E. Santopinto and A. Giachino, Phys. Rev. D **96**, 014014 (2017).
[32] A. Feijoo, V. K. Magas, A. Ramos, and E. Oset, Eur. Phys. J. C **76**, 446 (2016).
[33] J. X. Lu, E. Wang, J. J. Xie, L. S. Geng, and E. Oset, Phys. Rev. D **93**, 094009 (2016).
[34] C. W. Shen, J. J. Wu, and B. S. Zou, Phys. Rev. D **100**, 056006 (2019).
[35] R. Chen, J. He, and X. Liu, Chin. Phys. C **41**, 103105 (2017).
[36] B. Wang, L. Meng, and S. L. Zhu, Phys. Rev. D **101**, 034018 (2020).
[37] R. Aaij *et al.* (LHCb Collaboration), arXiv:2012.10380.
[38] H. X. Chen, W. Chen, X. Liu, and X. H. Liu, arXiv:2011.01079.
[39] Z. G. Wang, arXiv:2011.05102.
[40] K. Azizi, Y. Sarac, and H. Sundu, arXiv:2101.07850.
[41] U. Özdem, arXiv:2102.01996.
[42] F. Z. Peng, M. J. Yan, M. Sánchez Sánchez, and M. P. Valderrama, arXiv:2011.01915.
[43] R. Chen, Phys. Rev. D **103**, 054007 (2021).
[44] R. Chen, Eur. Phys. J. C **81**, 122 (2021).
[45] M. Z. Liu, Y. W. Pan, and L. S. Geng, Phys. Rev. D **103**, 034003 (2021).
[46] J. T. Zhu, L. Q. Song, and J. He, arXiv:2101.12441.
[47] W. Y. Liu, W. Hao, G. Y. Wang, Y. Y. Wang, E. Wang, and D. M. Li, Phys. Rev. D **103**, 034019 (2021).
[48] F. K. Guo, C. Hanhart, U.-G. Meißner, Q. Wang, Q. Zhao, and B. S. Zou, Rev. Mod. Phys. **90**, 015004 (2018).
[49] H. X. Chen, W. Chen, X. Liu, and S. L. Zhu, Phys. Rep. **639**, 1 (2016).
[50] X. K. Dong, F. K. Guo, and B. S. Zou, arXiv:2101.01021.
[51] X. K. Dong, F. K. Guo, and B. S. Zou, arXiv:2011.14517.
[52] J. J. Wu, L. Zhao, and B. S. Zou, Phys. Lett. B **709**, 70 (2012).
[53] T. Sekihara and T. Hyodo, Phys. Rev. C **87**, 045202 (2013).
[54] H. A. Ahmed and C. W. Xiao, Phys. Rev. D **101**, 094034 (2020).